Journal of Organometallic Chemistry, 217 (1981) 235—245
Elsevier Sequoia S.A., Lausanne — Printed in The Netherlands

A COMMENT ON THE STRUCTURES OF THE DODECACARBONYLS OF COBALT, RHODIUM AND IRIDIUM

D.L. KEPERT and S.C. WILLIAMS

School of Chemistry, The University of Western Australia, Nedlands, Western Australia, 6009 (Australia)

(Received March 4th, 1981)

Summary

The structures of [$Co_4(CO)_{12}$], [$Rh_4(CO)_{12}$] and [$Ir_4(CO)_{12}$] are considered from the viewpoint of electron pair repulsion theory. It is shown that the change from the icosahedral arrangement of ligands in the cobalt and rhodium compounds, to the cuboctahedral arrangement in the iridium compound, cannot be completely explained by the steric requirements of the M_4 cluster within the $(CO)_{12}$ polyhedron. It is necessary to invoke either an increase in metal—metal bonding in the iridium compound, or changes in metal—carbonyl bonding.

Introduction

The structures of [$Co_4(CO)_{12}$] [1], [$Rh_4(CO)_{12}$] [2] and [$Ir_4(CO)_{12}$] [3] are similar, each consisting of a tetrahedral arrangement of four metal atoms sur-

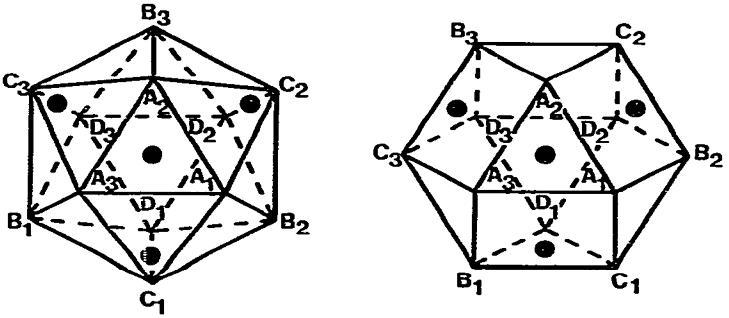

Fig. 1. (a) Icosahedral arrangement of twelve carbonyl groups around a tetrahedron of metal atoms. B_1, B_2 and B_3 are bridging atoms. (b) Cuboctahedral arrangement of twelve carbonyl groups around a tetrahedron of metal atoms. There are no bridging atoms.

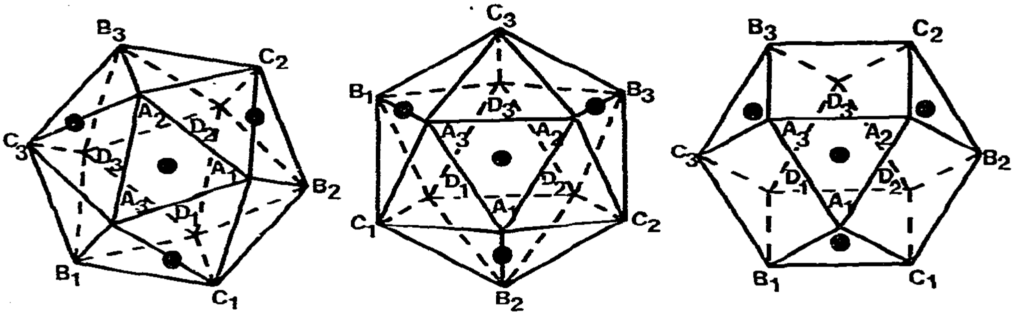

Fig. 2. (a) Icosahedral arrangement of twelve carbonyl groups around a tetrahedron of metal atoms. There are no bridging atoms. (b) Icosahedral arrangement of twelve carbonyl groups around a tetrahedron of metal atoms. C_1, C_2, C_3, D_1, D_2 and D_3 are bridging atoms. (c) Cuboctahedral arrangement of twelve carbonyl groups around a tetrahedron of metal atoms. D_1, D_2 and D_3 are bridging atoms.

rounded by twelve carbonyl groups. In the cobalt and rhodium compounds the carbonyl groups are arranged at the apices of an icosahedron (Fig. 1a) oriented so that three of the carbonyl groups (labelled B_1, B_2 and B_3 in Fig. 1a) are in bridging positions between pairs of metal atoms. In the iridium compound however, the carbonyl groups are at the vertices of a cuboctahedron, oriented so that each metal atom is bonded to three nonbridging ligands (Fig. 1b). In all molecules there is exact or a good approximation to three-fold symmetry, the three-fold axis being normal to the page in Figs. 1a and 1b. There has been considerable speculation concerning these structural differences. Albano, Ciani and Martinengo [4] using bonding considerations have argued that the lower ionization potentials of cobalt and rhodium will increase the metal-to-carbonyl π-bonding, stabilising the structure with bridging carbonyl groups. It should be noted however that both the icosahedron and the cuboctahedron can be oriented about a tetrahedron either with or without symmetrical bridging groups (Figs. 1 and 2).

On the other hand, Johnson and Benfield [5,6] have used the steric argument that the tetrahedral Co_4 and Rh_4 clusters, but not the larger Ir_4 cluster, can fit inside an icosahedral arrangement of carbonyl ligands provided the size of the icosahedron is determined by placing the carbonyl groups in contact, but it is not clear why this restriction should apply. That is, the expansion of the $[Co_4(CO)_{12}]$ polyhedron to the $[Ir_4(CO)_{12}]$ polyhedron is pictured as lengthening six of the 30 edges of an icosahedron to $\sqrt{2}$ of the previous value so that they become the diagonals of square faces of the cuboctahedron, with the length of the other 24 edges remaining constant. The alternative expansion of slightly lengthening all 30 edges with retention of the icosahedral geometry was not considered.

In contrast to these steric interactions between atoms, Gillespie [7] considers that the structures will be determined by the electron pair repulsion between both the metal—carbonyl and the metal—metal bonds. There are six metal—metal bonds required by the 18-electron rule which are assumed to be directed along each edge of the tetrahedron. However, no firm structural predictions were made.

In this work we extend these ideas using a more quantitative approach to electron pair repulsion theory. We have shown that this approach is very useful when considering the stereochemistry of compounds containing a shell of electrons around a single metal atom [8—12].

Calculations

The calculations follow previous work [8—12] and are based on the minimisation of the total repulsion energy, U, obtained by summing over all individual repulsion terms, u_{ij}. For the purposes of these repulsion energy calculations, the twelve repelling centres associated with the twelve carbonyl groups are situated at the vertices of a polyhedron. These repelling centres are the carbon atoms if the interactions are assumed to be purely ligand—ligand repulsions, or are somewhat displaced towards the metal atoms if the interactions are assumed to be electron pair repulsions. The nature of the repelling centres will be considered again later. The repulsion u_{ij} between two centres of repulsion, i and j, is assumed to be inversely proportional to some power n of the distance d_{ij} between them:

$$u_{ij} = a_n/d_{ij}^n$$

and

$$U = \sum_{ij} u_{ij} = a_n X$$

where a_n is the proportionality constant and X is the repulsion energy coefficient, which is a function of n and the geometry of the molecule. The most stable stereochemistry is simply calculated by the minimisation of X as a function of geometry. The geometries generated by this model are usually insensitive to the value chosen for n. In those cases where the results to depend on n, the best agreement with experiment is obtained for $n \sim 6$.

This method is similar to that used by Johnson and Benfield [6], except they have taken the distance between a pair of points on the surface of a sphere as directly proportional to the angle Ω_{ij} subtended at the centre of the sphere,

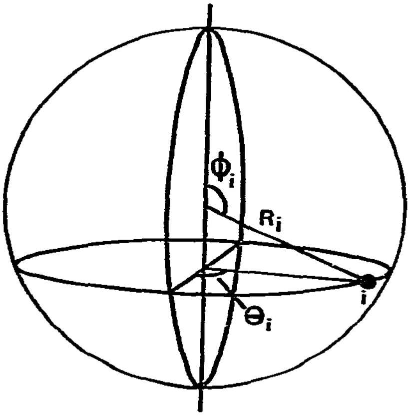

Fig. 3. Polar coordinates.

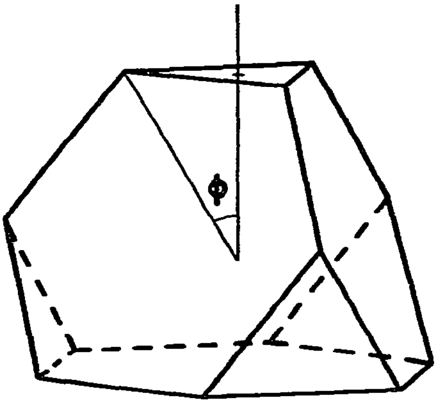

Fig. 4. Truncated tetrahedron.

rather than using the relation:

$$d_{ij} = 2\sin(\Omega_{ij}/2)$$

All results are presented in terms of polar coordinates about the centre of the molecule, as defined in Fig. 3.

[M(ligand)$_{12}$]

For purposes of comparison with the results from the [M$_4$(ligand)$_{12}$] calculations, it is convenient to first calculate the relative energies of the [M(ligand)$_{12}$] polyhedra. The polyhedra relevant to this work are the icosahedron, cuboctahedron, truncated tetrahedron and anticuboctahedron. The icosahedron is a regular polyhedron with all vertices identical, all faces equilateral triangles, and all edge lengths equal to 1.0515 r, where r is the radius of the polyhedron.

The cuboctahedron is a semiregular polyhedron containing both equilateral triangular and square faces, with all vertices identical and all edge lengths equal to 1.0000 r.

The truncated tetrahedron is another semiregular polyhedron with twelve identical vertices and is composed of equilateral triangular and hexagonal faces (Fig. 4). For the "hard sphere model", all edge lengths are equal to 0.8528 r, the hexagonal faces are regular, and the angle ϕ defined by Fig. 4 is equal to 30.0°. Depending on the form of the repulsion law, this "hard sphere" truncated tetrahedron distorts to a more favourable truncated tetrahedron by slightly increasing ϕ, increasing the size of the smaller triangular faces at the expense of the larger hexagonal faces.

The cuboctahedron in Fig. 5a can be considered to consist of a regular hexagonal arrangement of atoms DEFGHI coplanar with the central metal atom, with equilateral triangular arrangements of atoms above (ABC) and below (JKL) this plane. Rotation of the top half of the cuboctahedron by 60° relative to the bottom half forms the anticuboctahedron (Fig. 5b). The structure is defined by ϕ_A, the angle the ABCJKL metal—ligand bonds make with the three-

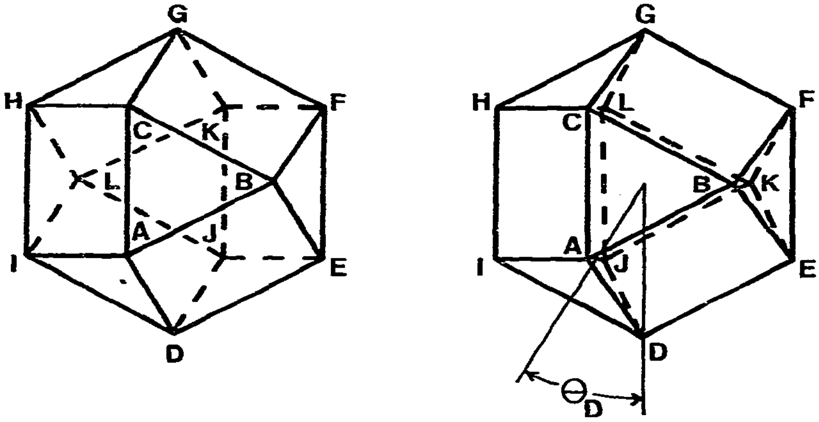

Fig. 5. Cuboctahedron and anticuboctahedron.

TABLE 1

REPULSION ENERGY COEFFICIENTS AND ANGULAR PARAMETERS FOR $[M(LIGAND)_{12}]$

		$u \alpha \frac{1}{d} n$			$u \alpha \frac{1}{\Omega} 6$
		$n = 1$	$n = 6$	$n = 12$	
Icosahedron	X	49.165	23.531	16.481	16.718
Anticuboctahedron	$\phi_A(^\circ)$	35.6	35.5	35.4	35.5
	$\theta_D(^\circ)$	32.2	31.1	30.8	31.3
	X	49.315	26.280	23.938	19.120
Cuboctahedron	X	49.342	26.483	24.222	19.288
Truncated Tetrahedron	$\phi\ (^\circ)$	31.8	30.5	30.1	30.5
	X	50.540	48.692	118.485	38.855

fold axis, and θ_D, which defines the shape of the central hexagon. For a hard sphere model, the edge lengths of the anticuboctahedron are the same as the cuboctahedron and equal to 1.0000 r. Significant distortions occur on going to the most favourable polyhedron, principally arising from a small increase in θ_D that increases the size of the eight triangular faces and decreases the size of the six larger square faces, turning them into trapezoids. If this distortion is allowed, the anticuboctahedron becomes more stable than the cuboctahedron, but if this distortion is not permitted the erroneous conclusion is reached that the anticuboctahedron is less stable than the cuboctahedron, as in Johnson and Benfield's work [6]. Such distortions are not possible for the cuboctahedron, as every edge is part of both a triangular face and a square face.

The repulsion energy coefficients for these polyhedra are collected in Table 1, calculated for $n = 1$, 6 and 12 in the repulsion law and for polyhedra radii of unity. Also shown are the results obtained using the Johnson and Benfield angular repulsion law.

$[M_4(ligand)_{12}]$

Two geometric models were used for the extension of these repulsion energy calculations to complexes of the type $[M_4(ligand)_{12}]$. Both models could be

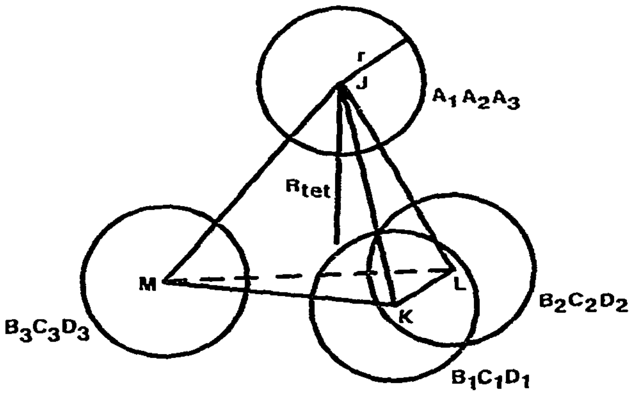

Fig. 6. General stereochemistry for the $[M(CO)_3]_4$ model.

modified by inclusion of interactions between the twelve polyhedral vertices and the six metal—metal bonds.

The $[M(CO)_3]_4$ *model.* In this model the compounds are considered to be composed of four $M(CO)_3$ fragments. Three polyhedral vertices are constrained to the surface of a sphere around each metal atom, the four metal atoms being placed at the corners of a regular tetrahedron (Fig. 6). The size of the tetrahedron is given by R_{tet} (Fig. 6) and the radius of the sphere about each metal atom is defined as r. A three-fold axis passes through metal atom J which generates the polyhedral vertices A_2 and A_3 about J from A_1. Similarly B_2, C_2 and D_2 about atom L and B_3, C_3 and D_3 about M are generated from B_1, C_1 and D_1 on atom K.

The $[M_4(CO)_{12}]$ *model.* The results from the $[M(CO)_3]_4$ model show that all twelve polyhedral vertices lie on the surface of a sphere centred about the centre of the M_4 tetrahedron. In the $[M_4(CO)_{12}]$ model, all polyhedral vertices were simply placed on the surface of a sphere of radius R_{poly} about the tetrahedron, with no particular linkage assumed between any carbonyl group and any metal atom. In the absence of any interaction with the metal—metal bonds, this model is the same as that described above for mononuclear complexes $[M(ligand)_{12}]$.

Results

The angular coordinates calculated from the first model, $[M(CO)_3]_4$ with no interactions from the metal—metal bonds, are shown in Fig. 7, obtained using $n = 6$ in the repulsion law. At low values of R_{tet}/r the twelve polyhedral ver-

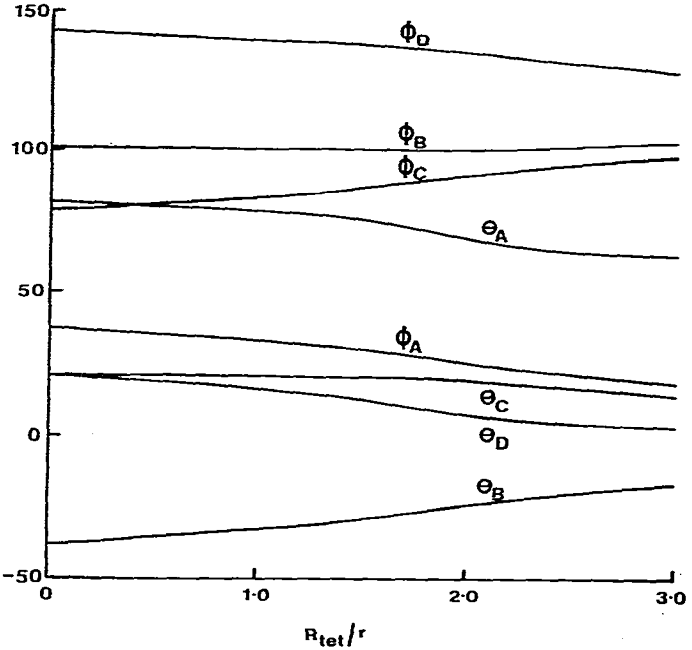

Fig. 7. Angular coordinates, in degrees, as a function of R_{tet}/r for $[M(CO)_3]_4$ with no contributions from metal—metal bonding, $n = 6$.

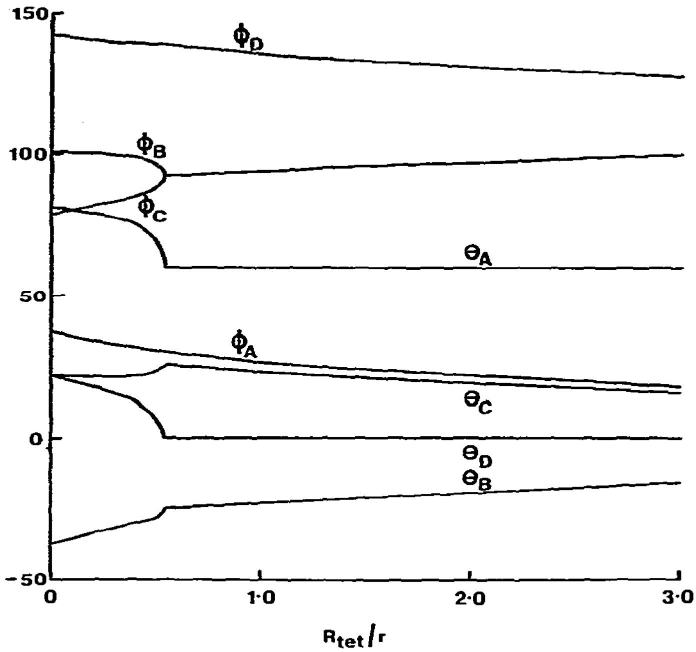

Fig. 8. Angular coordinates, in degrees, as a function of R_{tet}/r for $[M(CO)_3]_4$ with the inclusion of metal—metal bonding, $n = 6$.

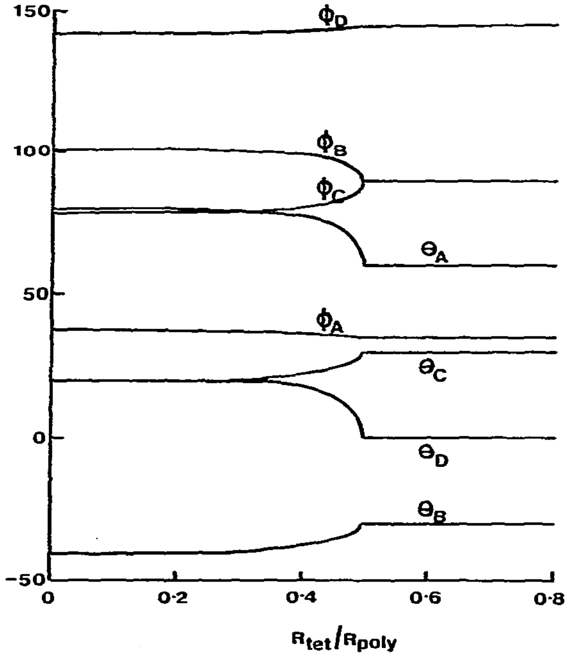

Fig. 9. Angular coordinates, in degrees, as a function of R_{tet}/R_{poly} for $[M_4(CO)_{12}]$ with the inclusion of metal—metal bonding, $n = 6$.

tices form an icosahedron as expected. However, the orientation of the icosahedron about the tetrahedron is not that shown in Fig. 1a, but is that shown in Fig. 2a. Each of the three metal atoms at the base of the tetrahedron is found to lie behind a face of the icosahedron, so that all carbonyl groups are non-bridging. As the radius of the tetrahedron is increased, the triangular faces $A_1A_2A_3$ and $B_iC_iD_i$ are rotated so that a cuboctahedron is formed. This gradual distortion toward the cuboctahedral stereochemistry occurs at lower values of R_{tet}/r as the value of n in the repulsion law is decreased [13]. A feature of these results is that all polyhedral vertices are equidistant from the centre of the polyhedron, although this is not required by the model.

These calculations can be modified by inclusion of electron pairs as repelling centres at the midpoint of each tetrahedral edge. If the repulsions from the metal—metal bonds and the metal—ligand bonds are weighted equally, the variation of angular parameters with R_{tet}/r is shown in Fig. 8. The results are qualitatively similar to those obtained previously, again corresponding to a continuous change from an icosahedron with no bridging carbonyl groups to a cuboctahedron with no bridging carbonyl groups. A comparison of Figs. 7 and 8 shows that the inclusion of metal—metal bonding into the model results in the cuboctahedral stereochemistry being attained at lower values of R_{tet}/r.

The angular coordinates derived from the second model, $[M_4(CO)_{12}]$ with the inclusion of metal—metal bonding, are shown in Fig. 9. As R_{tet}/r_{poly} is increased from zero, the stereochemistry again smoothly changes from an icosahedron with no bridging carbonyl groups until a cuboctahedron with no bridging carbonyl groups is attained at $R_{tet}/R_{poly} \sim 0.5$.

For purposes of comparison, calculations were also carried out with repulsions from the centres of the M_4 tetrahedral faces, rather than from the midpoints of the tetrahedral edges. In both models, $[M(CO)_3]_4$ and $[M_4(CO)_{12}]$, increasing R_{tet} resulted in the icosahedral structure with no bridging carbonyl groups being converted into a truncated tetrahedral structure with no bridging carbonyl groups. The four metal atoms are projected towards the triangular faces of the truncated tetrahedron, and the centres of the tetrahedral faces are aligned with the centres of the hexagonal faces of the truncated tetrahedron. The truncated tetrahedral stereochemistry is also obtained if four tetrahedrally placed metal atoms are considered to repel the twelve carbonyl groups, that is, if the twelve carbonyl groups are arranged to provide as large a hole as possible to accommodate the metal atoms. In this case it is the metal atoms rather than the electron pairs which are projected towards the hexagonal faces of the truncated tetrahedron.

Discussion

The results show that there is a smooth and continuous change in stereochemistry from an icosahedron to a cuboctahedron as the size of the metal tetrahedron is increased, as predicted by Johnson and Benfield [5,6]. However, two problems remain which are discussed in more detail below. Firstly, the changeover from the icosahedron to the cuboctahedron as R_{tet} is increased is much too gradual to explain the observed large structural differences if the repulsion energy simply originates from the carbon atoms. Secondly, the cal-

TABLE 2

STRUCTURAL PARAMETERS FOR $[M_4(CO)_{12}]$

	M = Co			M = Rh			M = Ir [a]		
	R(Å)	ϕ(°)	θ(°)	R(Å)	ϕ(°)	θ(°)	R(Å)	ϕ(°)	θ(°)
M_J	1.52	0.0	—	1.67	0.0	—	1.65	0.0	—
$M_{K,L,M}$ (av.)	1.52	110.0	0.0	1.67	108.5	0.0	1.65	109.7	0.0
C_A (av.)	2.90	35.2	54.9	3.16	33.4	59.8	3.36	32.0	61.4
C_B (av.)	2.33	99.5	300.8	2.27	101.0	300.4	3.05	92.2	332.6
C_C (av.)	3.02	78.0	—0.6	3.22	82.3	—1.1	3.10	91.2	27.9
C_D (av.)	2.93	138.2	0.0	3.34	135.3	0.6	3.12	143.8	4.7
R_{tet}	1.52			1.67			1.65		
r	1.92			1.97			1.87		
R_{tet}/r	0.79			0.85			0.88		
R_{poly}	2.80			3.00			3.16		
R_{tet}/R_{poly}	0.54			0.56			0.52		

[a] Ordered molecule in unit cell.

culated orientation of the $(CO)_{12}$ icosahedron about the M_4 tetrahedron is not that experimentally observed.

The experimental crystal structures, expressed as polar coordinates about the centre of the molecule, are summarised in Table 2, the values of R_{tet}, r and R_{poly} corresponding to the metal and carbon atoms. The experimental range of R_{tet}/r or R_{tet}/R_{poly}, is much too small to explain the gross changes in structure observed for the dodecacarbonyls, and it is necessary to include some differences in bonding between the three compounds. This could take one of three forms:

(i) The changeover to the cuboctahedron in the iridium compound can be brought about by an increase in metal—metal bonding along the tetrahedral edges. The midpoint of each tetrahedral edge lies beneath one of the square faces of the cuboctahedron, these being the least crowded parts of the molecule. This structural change is shown, for example, by comparison of Fig. 7 in which metal—metal bonds were assumed to be absent, with Fig. 8 in which the metal—metal bonds and metal—carbon bonds were equally weighted.

(ii) If the origin of the repulsion interaction lay not simply with the carbon atoms but with the metal—carbon bond, an increase in the σ-donation of the carbonyl group will decrease r and increase the tendency to form the cuboctahedral structure. That is, the increase in R_{tet}/r and the resulting cuboctahedral stereochemistry can be brought about by a decrease in r as well as by an increase in R_{tet}. A similar decrease in r will result from any decrease in metal-to-carbon π-bonding in the iridium compound.

(iii) As mentioned in the Introduction, Albano, Ciani and Martinengo [4] have suggested that the greater metal-to-carbonyl π-bonding in the cobalt and rhodium compounds will favour the formation of bridging carbonyl groups. The preference of the individual metal atoms is also indicated by the structure of $[Co_2Ir_2(CO)_{12}]$, which has the bridging icosahedral stereochemistry with one of the iridium atoms preferentially occupying the site containing no bridging carbonyl groups [4]. Bridging carbonyl groups can occur in an iridium cluster if some of the carbonyl groups are replaced by ligands with weaker π-acceptor

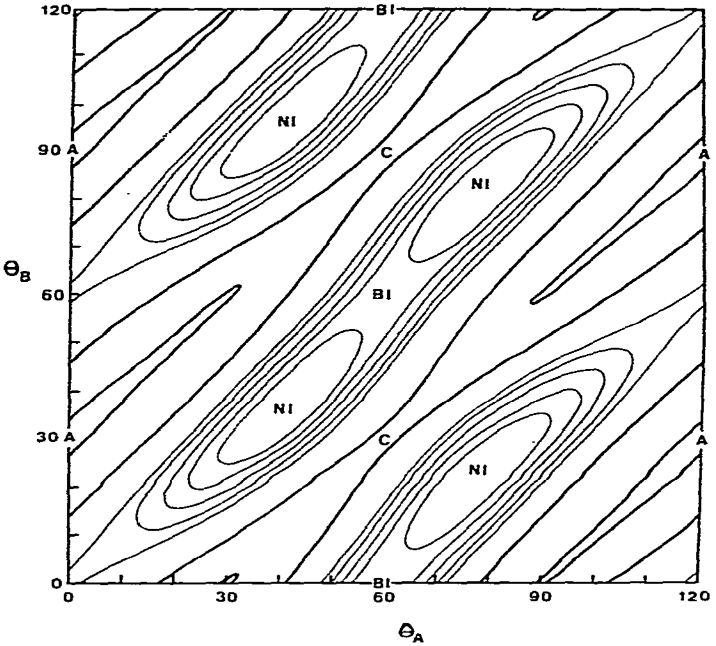

Fig. 10. Projection of the potential energy surface for $[M_4(\text{unidentate})_{12}]$ onto the θ_A—θ_B plane, in degrees. The five faint contour lines are for successive 0.1% increments above the minima, and the two heavy contour lines are for 1% and 2% increments above the minima, at NI. $R_{tet}/R_{poly} = 0.4$, $n = 6$.

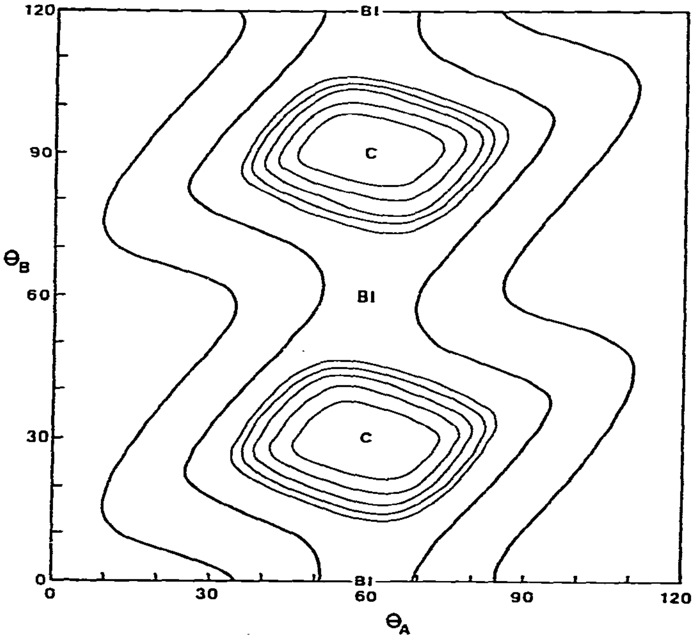

Fig. 11. Projection of the potential energy surface for $[M_4(\text{unidentate})_{12}]$ onto the θ_A—θ_B plane, in degrees. The five faint contour lines are for successive 0.1% increments above the minima, and the two heavy contour lines are for 1% and 2% increments above the minima, at C. $R_{tet}/R_{poly} = 0.5$, $n = 6$.

character, thereby strengthening the metal-to-ligand π-bonding of the remaining carbonyl groups. Thus [$Ir_4(CO)_{12}$] and [$Ir_4(CO)_{11}(CNBu)$] [14] contain no bridging groups, whereas [$Ir_4(CO)_{10}(PPh_3)_2$] [15], [$Ir_4(CO)_9(PPh_3)_3$] [15], [$Ir_4(CO)_{10}\{C_6H_4(AsMe_2)_2\}$] [16] and ($Ph_4P$)[$Ir_4(CO)_{11}Br$] [17] have bridging structures.

The relation between the different stereochemistries, particularly between the different orientations of the $(CO)_{12}$ icosahedron about the M_4 tetrahedron, can be illustrated by projecting the potential energy surface onto the θ_A—θ_B plane (Figs. 10 and 11).

The surface calculated for the [$M_4(CO)_{12}$] model with $R_{tet}/R_{poly} = 0.4$ is shown in Fig. 10. The icosahedron exists as a long valley running diagonally across the surface from $\theta_A = \theta_B = 0$ to $\theta_A = \theta_B = 90°$. Identical parallel valleys run through $\theta_A = 0$, $\theta_B = 60°$, and $\theta_A = 0$, $\theta_B = 120°$, and so on. The minima correspond to no bridging carbonyl groups (marked NI in Fig. 10), but these minima are separated by only a low saddle corresponding to the icosahedron with bridging carbonyl groups (marked BI in Fig. 10). Movement along this relatively flat valley corresponds to facile rotation of the ligand icosahedron about the metal tetrahedron. The highest points along the floot of these valleys (for example at $\theta_A = \theta_B = 0$) correspond to the icosahedral structure with six bridging carbonyl groups (Fig. 2b) which is not experimentally observed.

The high ridges separating the icosahedral valleys correspond to cuboctahedra, anticuboctahedra or intermediate structures. The lowest point on the ridge corresponds to a cuboctahedron with no bridging carbonyl groups (marked C in Fig. 10), whereas the highest points on the surface correspond to an anticuboctahedron with bridging carbonyl groups (marked A in Fig. 10). Movement along this ridge does not correspond to rotation of the complete cuboctahedron about the tetrahedron, and the cuboctahedron with bridging carbonyl groups (Fig. 2c) does not occur on this projection of the surface.

As R_{tet}/R_{poly} is increased to 0.5 (Fig. 11), the cuboctahedron with no bridging carbonyl groups exists as a relatively deep minimum. Two such minima are shown in Fig. 11, at $\theta_A = 60°$ and $\theta_B = 30°$ and $90°$, separated by a saddle at $\theta_A = \theta_B = 60°$ corresponding to the icosahedron with three bridging carbonyl groups.

References

1 C.H. Wei, Inorg. Chem., 8 (1969) 2384.
2 H. Carre, F.A. Cotton and B.A. Frenz, Inorg. Chem., 15 (1976) 380.
3 M.R. Churchill and J.P. Hutchinson, Inorg. Chem., 17 (1978) 3528.
4 V.G. Albano, P. Ciani and S. Martinengo, J. Organometal. Chem., 78 (1974) 265.
5 B.F.G. Johnson, J. Chem. Soc. Chem. Commun., (1976) 211.
6 B.F.G. Johnson and R.E. Benfield, J. Chem. Soc. Dalton Trans., (1980) 1743.
7 R.J. Gillespie, Chem. Soc. Revs., 8 (1979) 315.
8 D.L. Kepert, Prog. Inorg. Chem., 23 (1977) 1.
9 D.L. Kepert, Prog. Inorg. Chem., 24 (1978) 179.
10 D.L. Kepert, Prog. Inorg. Chem., 25 (1979) 41.
11 M.C. Favas and D.L. Kepert, Prog. Inorg. Chem., 27 (1980) 325.
12 M.C. Favas and D.L. Kepert, Prog. Inorg. Chem., 28 (1981) 309.
13 S. Williams, Honours Thesis, University of Western Australia, 1980.
14 M.R. Churchill and J.P. Hutchinson, Inorg. Chem., 18 (1979) 2451.
15 V. Albano, P.L. Bellon and V. Scatturin, J. Chem. Soc. Chem. Commun., (1967) 730.
16 M.R. Churchill and J.P. Hutchinson, Inorg. Chem., 19 (1980) 2765.
17 P. Chini, G. Ciani, L. Garlaschelli, M. Manessero, S. Martinengo, A. Sirona and F. Canziani, J. Organometal. Chem., 152 (1978) C35.